Received: 5 April 2021 | Accepted: 17 June 2021

DOI: 10.1111/ene.15001

european journal of neurology
the official journal of the european academy of neurology

ORIGINAL ARTICLE

Charcot–Marie–Tooth disease due to *MORC2* mutations in Spain

Rafael Sivera[1] | Vincenzo Lupo[2] | Marina Frasquet[3,4,5] | Herminia Argente-Escrig[3,4,5] | Jorge Alonso-Pérez[6,7] | Jordi Díaz-Manera[5,6,7,8] | Luis Querol[5,6,7] | María del Mar García-Romero[9,10] | Samuel Ignacio Pascual[9,10] | Tania García-Sobrino[11] | Carmen Paradas[12,13] | Juan Francisco Vázquez-Costa[3,4,5,15] | Nuria Muelas[3,4,5] | Elvira Millet[14] | Juan Jesús Vílchez[3,4,5,15] | Carmen Espinós[2] | Teresa Sevilla[3,4,5,15]

[1]Department of Neurology, Hospital Francesc de Borja, Gandía, Spain

[2]Unit of Rare Neurodegenerative Diseases Felipe, Centro de Investigación Príncipe, Valencia, Spain

[3]Neuromuscular Diseases Unit, Department of Neurology, Hospital Universitari i Politècnic La Fe, Valencia, Spain

[4]Neuromuscular and Ataxias Research Group, Instituto de Investigación Sanitaria La Fe, Valencia, Spain

[5]Centro de Investigación Biomédica en Red de Enfermedades Raras (CIBERER), Instituto de Salud Carlos III, Madrid, Spain

[6]Neuromuscular Diseases Unit, Department of Neurology, Hospital de la Santa Creu i Sant Pau, Barcelona, Spain

[7]Universitat Autonoma de Barcelona, Barcelona, Spain

[8]John Walton Muscular Dystrophy Research Center, Newcastle University Translational and Clinical Research Institute, Newcastle Upon Tyne, UK

[9]Neuropaediatrics Department, Hospital Universitario La Paz, Madrid, Spain

[10]Department of Pediatrics, Universidad Autónoma de Madrid, Madrid, Spain

[11]Department of Neurology, Complexo Hospitalario Universitario de Santiago de Compostela, Santiago de Compostela, Spain

[12]Department of Neurology, Hospital Universitario Virgen del Rocío, Sevilla, Spain

[13]Centro de Investigación Biomédica en Red de Enfermedades Neurodegenerativas (CIBERNED), Madrid, Spain

[14]Neuromuscular Diseases Unit, Department of Clinical Neurophysiology, Hospital Universitari i Politècnic La Fe, Valencia, Spain

[15]Department of Medicine, Universitat de València, Valencia, Spain

Correspondence
Teresa Sevilla, Hospital Universitari i Politècnic La Fe, Valencia, Centro de Investigación Biomédica en Red de Enfermedades Raras (CIBERER), Valencia, Universitat de Valencia, Avinguda de Fernando Abril Martorell, 106, 46026 València, Valencia.
Email: m.teresa.sevilla@uv.es

Funding information
This collaborative joint project is awarded by IRDiRC and funded by the Instituto de Salud Carlos III (ISCIII)—Subdirección General de Evaluación y Fomento de la Investigación within the framework of the National R+D+I Plan co-funded with ERDF funds (Grants PI16/00403, PI16/00316, PI19/01178) and Río Hortega contract to MF (Grant CM20/00152)

Abstract

Background and purpose: *MORC2* mutations have been described as a rare cause of axonal Charcot–Marie–Tooth disease (CMT2Z). The aim of this work was to determine the frequency and distribution of these mutations throughout Spain, to provide a comprehensive phenotypical description and, if possible, to establish a genotype–phenotype correlation.

Methods: Retrospectively, data on patients diagnosed with CMT2Z in Spain were collected and clinical, electrophysiological and muscle imaging information were analysed.

Results: Fifteen patients with CMT2Z were identified throughout Spain, seven of them belonging to a single kindred, whilst the rest were sporadic. The most common mutation was p.R252W, and four new mutations were identified. Eleven patients were categorized as having a scapuloperoneal phenotype, with asymmetric muscle weakness, early proximal upper limb involvement and frequent spontaneous muscular activity with distal

This is an open access article under the terms of the Creative Commons Attribution-NonCommercial License, which permits use, distribution and reproduction in any medium, provided the original work is properly cited and is not used for commercial purposes.
© 2021 The Authors. *European Journal of Neurology* published by John Wiley & Sons Ltd on behalf of European Academy of Neurology

and Juan Rodés contract to JFVC (Grant JR19/00030) and by the Generalitat Valenciana (Grant PROMETEO/2018/135 and PROMETEO/2019/075). Part of the equipment employed in this work has been funded by Generalitat Valenciana and co-financed with ERDF funds (OP ERDF of Comunitat Valenciana 2014-2020). TS is part of the Inherited Neuropathy Consortium (INC), which is within the NCATS Rare Diseases Clinical Research Network (RDCRN) and is supported also by the Muscular Dystrophy Association (MDA) and the Charcot–Marie–Tooth American Association (CMTA). MF, JD-M, LQ, CP, JFVC, NM, EM, JJV and TS are members of the European Reference Network for Rare Neuromuscular Diseases (ERN EURO-NMD).

sensory impairment and pes cavus, whilst two presented with a more classic length dependent sensory motor phenotype. This distinction was corroborated by the distribution of muscle fatty infiltration in muscle imaging. Two other patients were classified as having a neurodevelopmental phenotype consisting in congenital or early onset, delay in motor milestones, and global developmental delay in one of them. Nerve conduction studies revealed an unequivocally axonal neuropathy with frequent spontaneous activity, and serum creatine kinase levels were increased in 50% of the patients.

Conclusions: *MORC2* mutations are a rare cause of CMT in Spain, but in-depth phenotyping reveals a recognizable phenotypic spectrum that will be clinically relevant for future identification of this disease.

KEYWORDS
Charcot–Marie–Tooth disease, CMT2Z, *MORC2*, Spain

INTRODUCTION

Mutations in the gene microrchidia family CW-type zinc finger 2 (*MORC2*) were first identified as a rare cause of axonal Charcot–Marie–Tooth disease (CMT2Z) in three Spanish kindred [1]. Affected individuals in one family presented with hypotonia at birth, developmental delay, important limb weakness, scoliosis and respiratory insufficiency, whilst the rest presented with an axonal, motor and sensory asymmetric neuropathy with early proximal involvement. Almost simultaneously, the finding was replicated in four Australian families in which the phenotype also included pyramidal signs and occasionally learning difficulties, seizures or hearing defects [2]. Since then, several case reports and short clinical series have expanded and clarified the phenotypic spectrum to include cerebellar atrophy, respiratory insufficiency, dysphonia, microcephaly and retinal abnormalities [3–11]. Recently, *MORC2* mutations have been associated with growth retardation, short stature and cranial dysmorphism in many cases without prominent neuromuscular involvement [12]. To date, 18 causative amino acid changes in MORC2 have been reported, and there is clinical information of 89 patients, as detailed in Figure 1 and Table S1.

The MORC2 protein is a member of the MORC protein family and has a GHKL-type ATPase module composed of a GHKL-type

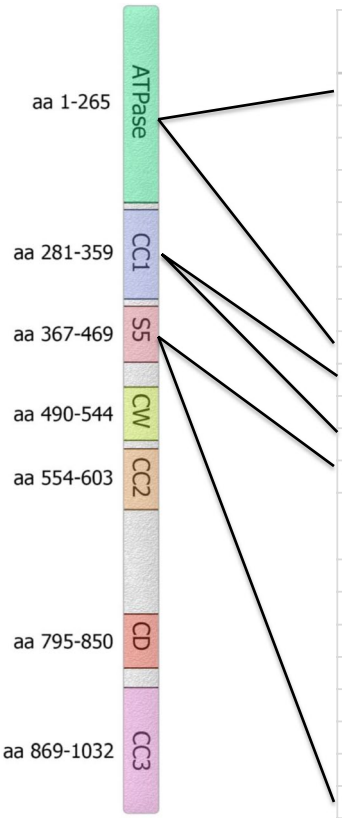

MORC2 Mutation	Phenotype	Reference
p.T24I	Neurodevelopmental	12
p.E27K	Neurodevelopmental	12
p.S87L	Neurodevelopmental	1
p.A88V	Neurodevelopmental	12
p.R132C	Neurodevelopmental	12
p.R132L	Scapuloperoneal	4
p.A152P	SM polyneuropathy	This work
p.E236G	Scapuloperoneal	2
p.R252W	Scapuloperoneal	1
p.R266S	Neurodevelopmental	12
p.R319H	Adult onset SMA	11
p.R319C	SM polyneuropathy	This work
p.S388R	Neurodevelopmental	12
p.Y394C	Neurodevelopmental, scapuloperoneal	10
p.Q400R	Scapuloperoneal	5
p.A406V	Scapuloperoneal	This work
p.C407Y	SM polyneuropathy	10
p.V413F	Neurodevelopmental	12
p.T424R	Neurodevelopmental	6
p.A431V	Scapuloperoneal	10
p.D466N	Scapuloperoneal	7
p.D466G	Scapuloperoneal	This work

FIGURE 1 MORC2 protein structure and corresponding *MORC2* mutations and reported phenotype. CC, coiled-coil insertion; CW, zinc finger domain; CD, coil domain; SMA, spinal muscular atrophy [Colour figure can be viewed at wileyonlinelibrary.com]

14681331, 2021, 9, Downloaded from https://onlinelibrary.wiley.com/doi/10.1111/ene.15001 by Readcube (Labtiva Inc.), Wiley Online Library on [26/06/2023]. See the Terms and Conditions (https://onlinelibrary.wiley.com/terms-and-conditions) on Wiley Online Library for rules of use; OA articles are governed by the applicable Creative Commons License

ATPase domain (residues 1–265), a transducer S5-like domain (residues 366–494) and a coiled-coil insertion CC1 (residues 282–361), a CW-type finger domain, and three predicted coiled-coil domains [13,14]. Causative mutations have been detected in all the domains that compose the ATPase module. The most frequent location is the GHL-ATPase domain, where the c.754C>T (p.R252W) change can be found, which represents 41% of the cases published. The pathway by which these changes alter the function of MORC2 and can cause peripheral neuropathy has been subject to much debate and many investigations and includes transcriptional dysregulation, HUSH-mediated repression, destabilization of the ATPase-CW module, altered expression of homeobox genes etc. [15,16]. There does not seem to be a clear correlation between the affected domain and the phenotype, although most of the variants have been detected in very few subjects (Figure 1, Table S1).

The aim of the study was to determine the distribution and frequency of causative *MORC2* mutations in Spain, to provide a comprehensive phenotypical description and to try to establish a genotype–phenotype correlation.

PATIENTS AND METHODS

Patients

This cross-sectional retrospective observational study includes all CMT patients with causative *MORC2* mutations evaluated at five centres throughout Spain. Patients were identified in a nationwide register of hereditary neuropathies developed in 2012 as part of the Spanish Registry of Neuromuscular Diseases project which was designed in accordance with current Spanish law on biomedical research and data protection. The Registry is reviewed annually to safeguard the quality of the information and data included in the Registry have been used in previous published studies. Also, a call for collaboration was issued in the Neuromuscular Work Group of the Spanish Neurology Society and the genetic database of Centro de Investigación Principe Felipe (CIPF) in Valencia was reviewed.

Standard protocol approvals, registrations and patient consents

All patients and relatives included in the present study signed informed consent, and the research protocols were approved by the respective institutional board of the Ethics Committees of the corresponding hospitals. Photographs and videos of the patients were taken and reproduced only after specific informed consent.

Genetic studies

In all cases the molecular studies were performed in the CIPF in Valencia. The *MORC2* mutations of the first kindred were studied with whole exome sequencing as previously reported [1]. Two additional families were then diagnosed by Sanger sequencing [1]. A search for mutations in *MORC2* using an in-house gene panel that employs a hybridization-based targeted sequencing with Agilent probes (Agilent technologies) to capture the coding exons and flanking intronic sequences of 121 inherited peripheral neuropathy genes (Table S2) and sequencing on an Illumina MiSeq was performed in the rest of the cases. Variant analysis from next generation sequencing data was carried out using standard procedures. For a comprehensive impact analysis of the novel variants, VarSome (https://varsome.com/) which evaluates them according to the American College of Medical Genetics guidelines was used [17]. Genotype–phenotype correlation and final classification of the variants were discussed in a multidisciplinary setting including CMT clinicians and a geneticist specialized in inherited peripheral neuropathies. All the variants reported in this work were confirmed by Sanger sequencing and further investigated by segregation analysis if possible.

Clinical assessments

Clinical assessments were collected using a standardized history and symptom questionnaire. Examinations included strength using the standard Medical Research Council (MRC) scale, pinprick, vibratory and positional sensory modalities, reflexes, as well as a general and neurological examination. The severity of the neuropathy was evaluated with the CMT neuropathy score version 1 (CMTNSv1) as a significant proportion of these patients had not undergone the neurophysiological radial nerve testing which is mandatory for the second version [18,19]. The CMT examination score was used for patients without nerve conduction studies.

Nerve conduction studies

Motor and sensory nerve conduction velocities (CVs) were performed using standard techniques. Temperature was controlled during the procedure and kept at more than 32°C. Compound muscle action potential amplitudes (CMAPs), sensory nerve action potential amplitudes (SNAPs), conduction velocities and distal latencies were recorded. Needle electromyography was performed in proximal and distal muscles of the upper and lower limbs. Spontaneous muscular activity was graded from 0 to ++++; motor unit potential amplitude, duration and phases were analysed.

Muscle magnetic resonance imaging

Muscle magnetic resonance imaging (MRI) was performed in the upper and lower limbs if possible. The protocol employed was the same as described previously, and muscle fatty substitution was graded from 0 to 4 according to the modified Mercuri score as

14681331, 2021, 9, Downloaded from https://onlinelibrary.wiley.com/doi/10.1111/ene.15001 by Readcube (Labtiva Inc.), Wiley Online Library on [26/06/2023]. See the Terms and Conditions (https://onlinelibrary.wiley.com/terms-and-conditions) on Wiley Online Library for rules of use; OA articles are governed by the applicable Creative Commons License

follows: 0, no fat signal in muscle; 1, traces of increased signal intensity on the T1-weighted MRI sequences; 2, increased T1-weighted signal intensity with beginning confluence in less than 50% of the muscle; 3, increased T1-weighted signal intensity with beginning confluence in more than 50% of the muscle; 4, entire muscle replaced by increased density of connective tissue and fat [20,21]. Heat maps of muscle fatty infiltration were developed.

Laboratory analysis

Blood tests were performed after overnight fasting and at least 5 days without any physical exertion. They included basic biochemical analysis and creatine kinase (CK) activity in the serum. The upper limit CK levels were defined by each laboratory and hyperCKemia was considered when the value was >1.5 times the upper limit of normal according to the European Federation of Neurological Societies guidelines [22]. Median CK values were determined if more than one was available.

RESULTS

Genetic analysis

A total of seven *MORC2* missense mutations were identified in nine families with CMT (Table 1). All the genetic studies were performed in the CIPF in Valencia. 389 CMT2 probands had to be screened to detect these subjects; in most of them causative *GDAP1*, *GJB1* and *MFN* changes had already been ruled out. The most common change was the NM_001303257:c.754C>T (p.R252W), which was detected in a seven-member kindred and in two sporadic patients. Two other previously reported mutations were observed, the NM_001303257:c.260C>T (p.S87L) and the NM_001303257:c.1181A>G (p.Y394C) [1,10,12].

The other four variants were detected for the first time in this work: the NM_001303257:c.955C>T (p.R319C) and NM_001303257:c.1397A>G (p.D466G) changes were predicted as deleterious by eight different pathogenic predictions in the VarSome platform and, moreover, they are located in the same codon where previous pathogenic mutations have been reported (p.R319H and p.D466N, respectively) [7,11]; the NM_001303257:c.1217C>T (p.A406V) mutation was predicted as deleterious by five different computational predictions and it segregates with the disease—the affected father harboured the variant in heterozygous state whilst two healthy siblings were negative for this change. Therefore, the novel missense changes p.R319C, p.D466G and p.A406V were considered as new *MORC2* pathogenic mutations. Finally, the NM_001303257:c.455C>G (p.A152P) variant was predicted as benign by 11 *in silico* programs in VarSome and it appears in 1/250364 alleles in the gnomAD database (https://gnomad.broadinstitute.org/); no other family members were available for segregation analysis. Thus it was classified as a variant of uncertain significance (VUS).

Clinical picture

Fifteen CMT2Z patients were included, and the clinical characteristics of 14 are detailed in Table 1. Part of the clinical information of families fCMT-197, fCMT-237 and fCMT-438 have been previously reported but are detailed and updated in this work [1]. Probands were detected throughout Spain, without a clear geographical cluster.

To categorize the clinical characteristics into phenotypic groups, whether the predominant impairment was neurodevelopmental or neuromuscular was taken into account, and in the latter case whether muscle weakness was length dependent or asymmetric with early shoulder girdle involvement.

The 11 patients with the p.R252W, p.A406V and p.D466G changes were classified as having a scapuloperoneal phenotype, reminiscent of the description published by Davidenkow in 1927 [23]. Symptom onset appeared in the first two decades except for one asymptomatic 17-year-old carrier. The most frequent initial symptoms were walking difficulties, tripping and cramps, the former present in 78%. Weakness always began distally in the lower limbs but spread to intrinsic hand muscles (usually between 20 and 30 years of age) and subsequently to proximal muscles of the upper more than the lower limbs. Proximal muscle involvement was heterogeneous, weakness being more prominent in pelvic and especially in shoulder girdle muscles, whilst knee and elbow extensors were relatively preserved (mean MRC scores of shoulder abduction vs. elbow flexo-extension were 3.2 vs. 4.1), as seen in Figure 2. Neck extension was weak in 6/10 patients. Spontaneous muscular activity was frequently observed, mostly in shoulder girdle muscles (Videos S1–S3) but also in other areas like the thigh muscles or even the tongue of patient III:3 of fCMT-397 (Video S4). Distal limb sensory impairment was observed early in the course of the disease, as were pes cavus and reduced tendon reflexes. Two patients reported hearing loss, and the two most severely affected also reported urinary incontinence. No central nervous system features were observed, like pyramidal signs, learning difficulties or seizures.

The cases harbouring the p.R319C and p.A152P changes were classified as having a sensory-motor length dependent polyneuropathy phenotype. Patient S1247, harbouring the p.R319C change, reported an onset at 30 years with stumbling and distal lower limb weakness. Mild proximal weakness in the lower limbs appeared during the course of the disease, as well as in the intrinsic hand muscles but not in the shoulder girdle. Sensory impairment was prominent, especially in the lower limbs needing a walker for stable ambulation, and tendon reflexes were asymmetrically reduced. Finally, patient S1238 (p.A152P—VUS) had a disease onset in the first decade with stumbling, foot deformities and distal lower limb weakness. Disease progression was relatively slow until the fifth or sixth decade, with clear worsening of the distal weakness and development of intrinsic hand muscles, and proximal lower limb weakness but no proximal upper limb weakness. All sensory modalities were impaired throughout the disease. Pes cavus, scoliosis and upper limb tremor were observed.

14681331, 2021, 9, Downloaded from https://onlinelibrary.wiley.com/doi/10.1111/ene.15001 by Readcube (Labtiva Inc.), Wiley Online Library on [26/06/2023]. See the Terms and Conditions (https://onlinelibrary.wiley.com/terms-and-conditions) on Wiley Online Library for rules of use; OA articles are governed by the applicable Creative Commons License

TABLE 1 Clinical characteristics.

Patient	*MORC2* mutation	Phenotype	Onset (years)	Cramps	Age	Motor		Sensory		Reflexes		CMTNS CMTES	Functional situation (#)	CK	Other
						UL	LL	UL	LL	UL	LL				
fCMT-438	p.S87L	ND	Hypotonia at birth	No	6	3/3	4/2	–	–	0	0	–/–	Wheelchair	–	Microcephaly, scoliosis
fCMT-237 II:1	p.R252W	SP	Stumbling, LL weakness (5–10)	–	41	2/2	3/2	T, P, V	T, P, V	0	0	30/22	Wheelchair (58)	–	
fCMT-237 II:3	p.R252W	SP	Difficulty walking, cramps (5)	Yes	75	2/2	2/2	T, P, V	All	0	0	31/28	Wheelchair (60)	219	Incontinence, hypoacusis
fCMT-237 III:1	p.R252W	SP	Difficulty walking, cramps (3)	Yes	47	4/3	4/2	T, P, V	T, P, V	0	0	24/20	Walking stick (31)	381	Incontinence, tremor
fCMT-237 III:4	p.R252W	SP	LL weakness (16)	Yes	51	4/2	4/2	T, P, V	T, P, V	0	0	27/22	Walking stick (35)	118	
fCMT-237 IV:3	p.R252W	SP	Cramps (5)	Yes	20	5/4	5/4	V	P, V	+	0	11/9	Running difficulty	–	
fCMT-237 IV:4	p.R252W	SP	Asymptomatic, mild cramps	Yes	17	5/5	5/4	Normal	V	++	Achilles 0 Patellar +	–/2	Difficulty heel walking	–	
fCMT-197	p.R252W	SP	Delay motor milestones (2)	Yes	45	2/2	2/2	T, P, V	T, P, V	0	0	32/29	Wheelchair (39)	210	Incontinence
fCMT-40	p.R252W	SP	Stumbling (5)	Yes	26	5/4	5/2	N	T	0	0	9/7	No aids	804	
S1247	p.R319C	SMP	Stumbling, LL weakness (30)	Yes	65	5/4-	4/2	T, P, V	All	Left 0 right +	0	23/21	Walker (65)	350	
S1325	p.Y394C	ND	Delay motor and mental development	No	46	4/3	2/2	Normal	P, V	0	0	25/18	Wheelchair (36)	–	Intellectual disability
fCMT-397	p.A406V	SP	LL weakness, cramps (13)	Yes	45	2/3	3/4	Normal	T, P, V	0	0	18/15	Wheelchair (45)	555	
S1150	p.D466G	SP	Proximal LL weakness (25)	No	68	2/3	2/0	T, P, V	T, P, V	0	0	22/18	Walker (58)	–	Hyperhidrosis, tremor
S1238	p.A152P[a]	SMP	Stumbling, foot deformities (5–10)	Yes	75	5/4	4/4	–	All	0	0	15/13	Crutches (60)	246	Tremor, scoliosis

Abbreviations: #, age at which the aid use started; CK, maximum creatine kinase in serum expressed in U/l; CMT, Charcot–Marie–Tooth; CMTNS, CMT neuropathy score version 1; CMTES: CMT examination score; LL, lower limbs; ND, neurodevelopmental phenotype; SMP, sensory motor length dependent polyneuropathy; SP, scapuloperoneal phenotype; UL, upper limbs.

Sensory modalities: P, pain; Po, positional; T, touch; V, vibration.

[a]This change is classified as a variant of uncertain significance at the moment.

14681331, 2021, 9, Downloaded from https://onlinelibrary.wiley.com/doi/10.1111/ene.15001 by Readcube (Labtiva Inc.), Wiley Online Library on [26/06/2023]. See the Terms and Conditions (https://onlinelibrary.wiley.com/terms-and-conditions) on Wiley Online Library for rules of use; OA articles are governed by the applicable Creative Commons License

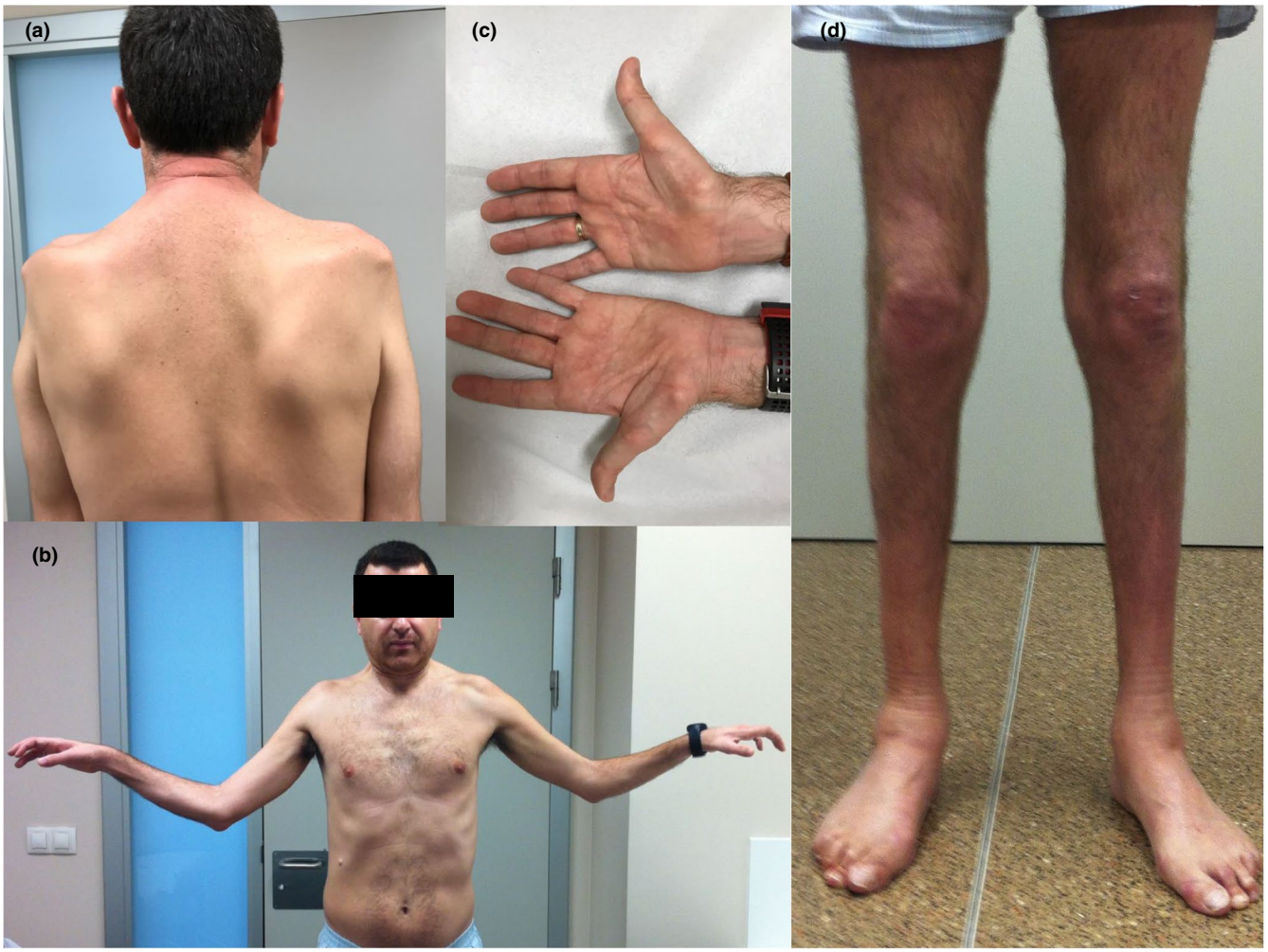

FIGURE 2 Characteristic 'scapuloperoneal' phenotype in patient fCMT-397 at age 44. (a) Asymmetric scapular winging and atrophy of trapezius and deltoideus. (b) Patient is incapable of raising his arms over his shoulders because of weakness of the scapular girdle muscles. (c) Hand atrophy, especially in thenar muscles. (d) Bilateral atrophy of the lower legs [Colour figure can be viewed at wileyonlinelibrary.com]

The patients harbouring the p.S87L and p.Y394C changes were classified as having a neurodevelopmental disorder phenotype. The patient with the p.Y394C change (S1325) had an onset in early childhood consisting in developmental motor and cognitive delay. He managed to walk at a late age, but proximal weakness appeared in his 30s and soon after he became wheelchair bound. At examination there was important lower limb weakness (2/5 proximally and distally) and upper limb involvement (4/5 proximally and 2–3/5 distally) with mild asymmetry. Intellectual disability was also prominent, but no seizures, microcephaly or facial dysmorphism were observed. Patient III:3 of fCMT-438, harbouring the p.S87L mutation, presented with hypotonia at birth and was able to stand up at 24 months as was reported previously [1]. At 6 years of age, she is wheelchair dependent but able to take a few lateral steps, and on examination there is prominent neck and limb girdle weakness (3/5 global MRC score) as well as of the distal muscles of the limbs, with relative sparing of knee and elbow flexion-extension (4/5). She also suffers from kyphoscoliosis treated with a corset, needs nutritional supplementation and occasional respiratory support. Microcephaly was detected at birth, but subsequent cognitive and language development has been practically normal.

Electrophysiological studies

Nerve conduction studies and needle electromyography were performed in 13 patients and the findings are presented in Table 2. Changes were relatively uniform in all phenotypic groups. Motor and sensory CVs were within normal range in practically all the nerves that were explored. CMAPs were reduced globally, but especially in the lower limb nerves. SNAPs were also decreased throughout the whole series, even when studied early in the course of the disease. In most patients, the decrease in CMAPs was not homogeneous amongst the different nerves of the upper and lower limbs. The median nerve appeared to be affected earlier and to a greater degree than the ulnar nerve: mean median CMAP was 4 mV (0.1–8 mV) and mean ulnar CMAP was 7.9 mV (0.5–15.5 mV). In the

14681331, 2021, 9, Downloaded from https://onlinelibrary.wiley.com/doi/10.1111/ene.15001 by Readcube (Labtiva Inc.), Wiley Online Library on [26/06/2023]. See the Terms and Conditions (https://onlinelibrary.wiley.com/terms-and-conditions) on Wiley Online Library for rules of use; OA articles are governed by the applicable Creative Commons License

TABLE 2 Nerve conduction studies

Patient	*MORC2* mutation	Age	Ulnar CV/ CMAP	Median CV/ CMAP	Peroneal CV/CMAP	Posterior tibial CV/ CMAP	Ulnar CV/ SNAP	Median CV/SNAP	Sural CV/ SNAP	Peroneal CV/SNAP	Needle electromyography		
											Spontaneous activity	Distribution	MUP morphology
fCMT-438	p.S87L	2	–	–	31.7/0.7	–	–	–	56/3.3	–	–	–	Denervation
fCMT-237 II:1	p.R252W	41	–	NR	NR	–	–	NR	NR	–	Fa	Biceps, deltoid	Increased A, P
fCMT-237 II:3	p.R252W	75	58/4.5	–	NR	–	55/1.2	–	NR	–	Fi, PSW	Triceps	Increased A, P, D
fCMT-237 III:1	p.R252W	47	61.7/10	55/7.8	43.3/0.7	47.6/13.4	NR	NR	NR	NR	Fa +, M +++	AT, ADM	Increased A, P, D
fCMT-237 III:4	p.R252W	51	58/4.3	NR/2.2	37/2.3	42.5/5.2	–	NR	NR	–	No	–	Increased A, P
fCMT-237 IV:3	p.R252W	20	54.7/8.2	55/6.6	46.8/3.5	50/10.3	53.6/3.1	NR	52/1.2	NR	Fa ++, M ++	Deltoid, ADM, AT	Increased A, P, D
fCMT-197	p.R252W	22	62/15.5	56/8	57/0.7	42/8.4	46/0.7	NR	39/0.8	NR	M +, Fi ++, PSW ++	Deltoid, biceps, ADM, AT	Increased A, P, D
fCMT-440	p.R252W	25	–	57.8/12	NR	–	52/2.3	52/4.6	NR	–	–	–	–
S1247	p.R319C	64	50/7.1	NR/0.4	NR/0.1	NR	45.8/3.8	35.6/0.8	42/1	38.3/0.9	Fi +, PSW +	AT	Increased A, P, D
S1325	p.Y394C	45	–/0.5	NR	–	–	NR	–	–	–	–	–	–
fCMT-397	p.A406V	38	65/11	66.7/0.1	28.6/0.4	48.2/4.2	57/0.3	51.6/1	NR	NR	Fa +, M +, Fi +	Deltoid, ADM, Ga, gluteus	Increased A, P, D
S1150	p.D466G	47	56/4.6	49/1.3	–	–	NR	NR	–	–	PSW +	Biceps, AT	Increased A, P, D
S1238	p.A152P[a]	75	37/10	42/5.6	36/0.6	34/0.9	36/9	37/13	31/4	–	Fi ++, PSW ++	AT, Ga	Increased A, P, D

Abbreviations: –, not performed; A, amplitude; ADM, abductor digiti minimi; AT, anterior tibialis; CMAP, compound muscle action potential, expressed in mV; CV, conduction velocity, expressed in m/s; D, duration; Fa, fasciculation; Fi, fibrillation; Ga, gastrocnemius; M, myokymia; MUP, motor unit potential; NR, not recordable; P, polyphasia; PSW, positive sharp wave; SNAP, sensory nerve action potential, expressed in mV.

[a]This change is classified as a variant of uncertain significance at the moment.

14681331, 2021, 9, Downloaded from https://onlinelibrary.wiley.com/doi/10.1111/ene.15001 by Readcube (Labtiva Inc.), Wiley Online Library on [26/06/2023]. See the Terms and Conditions (https://onlinelibrary.wiley.com/terms-and-conditions) on Wiley Online Library for rules of use; OA articles are governed by the applicable Creative Commons License

lower limbs, there was also asymmetry between the CMAPs of the more affected peroneal nerve and the tibial nerve. Needle electromyography was performed in 11 patients and spontaneous muscular activity was detected in nine, consisting mostly of fibrillation and positive sharp waves, but also fasciculations and myokymia. They were prominent in the upper limb muscles (deltoideus, biceps, abductor digiti minimi) but also present in lower limb muscles of 4/9 patients. Motor unit potentials were unequivocally classified as neurogenic, with increase in amplitude, duration and number of phases.

Muscle magnetic resonance

Muscle MRI was performed in seven patients; the images of fCMT-237 III:4 and fCMT-197 can be consulted in previous work, and of fCMT-237 III:1 and fCMT-397 in Figure 3 [1]. All studies were performed in patients with a scapuloperoneal clinical presentation except S1247 and in all the studied subjects there was detectable muscle fatty infiltration and atrophy. Short T1 inversion recovery hyperintensities were only observed in the gastrocnemius of one patient. Heat maps of fatty substitution are detailed in Figure 3b. In patients with the scapuloperoneal phenotype the pattern of muscle fatty infiltration was not length dependent as the intrinsic muscles of the feet were less infiltrated than the muscles of the calf in 4/5 cases (Figure 3a). In the latter, there was less fatty infiltration in the deep posterior compartment of the calf compared to the rest of the compartments (graded 2.4 vs. 3.4 with the modified Mercuri scale). In the thigh, early and frequent fatty substitution in semimembranosus and semitendinosus muscles could be detected, and in the

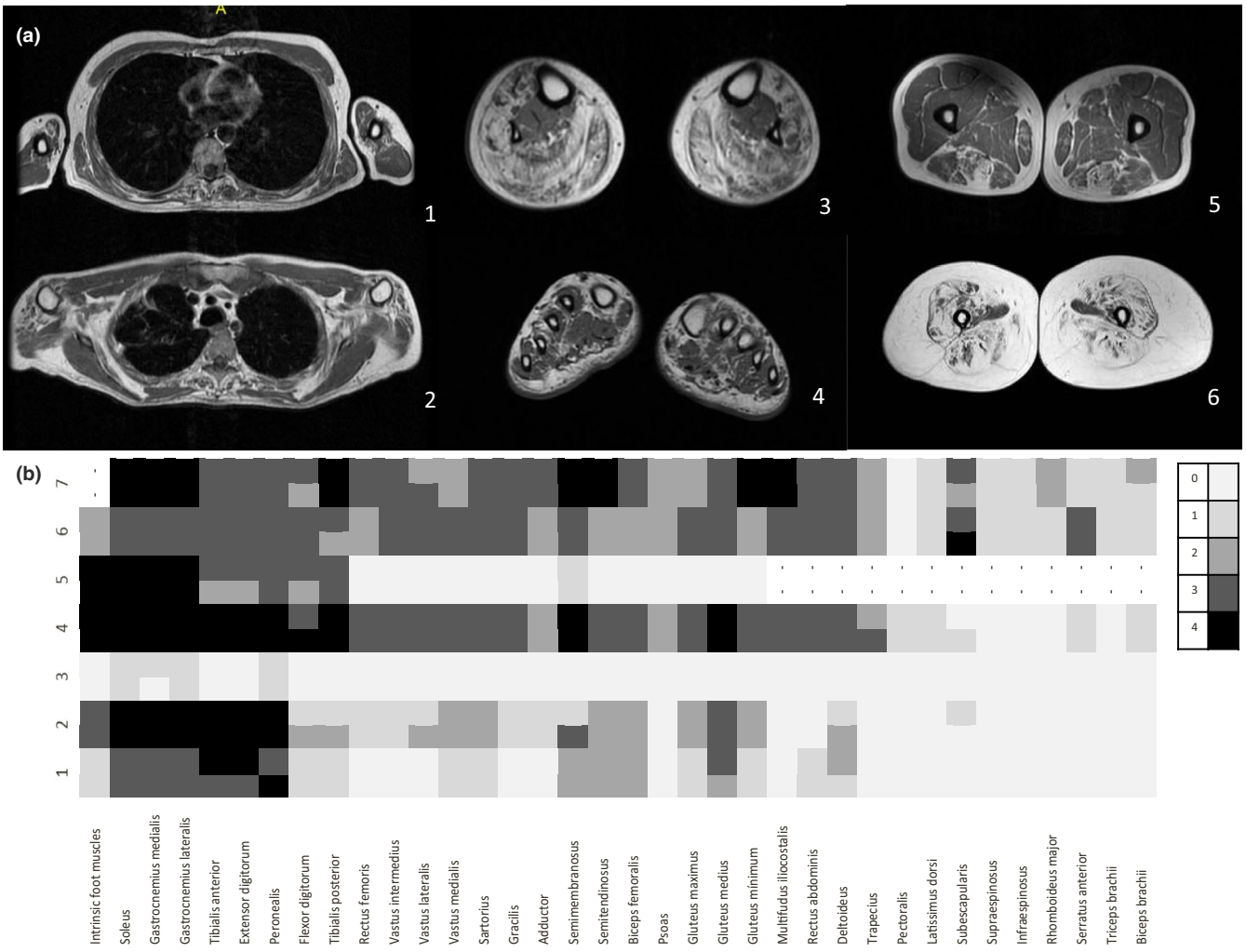

FIGURE 3 (a) (1), (2) Scapular girdle and upper limb muscle MRI of patient III:3 fCMT-397 at age 38. Note the atrophy and fatty infiltration in the serratus anterior, triceps and biceps brachii [1] as well as in the deltoideus and subscapularis [2]. (a) (3), (4), (5) Lower limb muscle MRI of patient fCMT-237 III:1 at age 48. In the calf there is relative preservation of the deep posterior muscular compartment of the calf and the intrinsic foot muscles compared to the superficial posterior and antero-lateral compartments. In the thigh, note the initial fatty infiltration in the semimembranosus and semitendinosus muscles. (6) Thigh muscle MRI of patient S1150, age 69, with prominent fatty infiltration of all muscles except the adductor longus. (b) Heat map showing muscle imaging involvement by muscle MRI: (1) fCMT-237 III:1, age 48, p.R252W; (2) fCMT-237 III:4, age 51, p.R252W; (3) fCMT-237 IV:3, age 20, p.R252W; (4) fCMT-197, age 45, p.R252W; (5) S1247, age 64, p.R319C; (6) fCMT-397 III:3, age 38, p.A406V; (7) S1150, age 69, p.D466G. In each patient fatty substitution is graded 0–4 on the right and left side. –, not performed

14681331, 2021, 9, Downloaded from https://onlinelibrary.wiley.com/doi/10.1111/ene.15001 by Readcube (Labtiva Inc.), Wiley Online Library on [26/06/2023]. See the Terms and Conditions (https://onlinelibrary.wiley.com/terms-and-conditions) on Wiley Online Library for rules of use; OA articles are governed by the applicable Creative Commons License

latter stages of the disease there was relative preservation of the adductor muscles, especially the adductor longus. In the pelvic girdle muscles, the gluteus medius and minimus were frequently infiltrated, as were the deltoideus, trapecius and subescapularis in the shoulder girdle, but the forearm and hand muscles were not studied. Left–right asymmetry, although mild, was present in all the studies performed. These findings correlated with abnormal muscular strength on clinical examination in all cases. The muscle MRI performed in subject S1247 confirmed the clinical length dependent weakness with an almost exclusive fatty infiltration of distal muscles without proximal involvement except for the semimembranosus.

HyperCkemia

Creatine kinase serum levels were determined in eight patients and values are shown in Table 1. The mean values for blood CK were increased (360.4 mg/dl, range 118–804 mg/dl). CK levels did not correlate with clinical phenotype, severity or disease progression; in fact the highest levels were detected in a young patient (26 years) with a mild-to-moderate phenotype (CMTNS 15).

DISCUSSION

Here a compilation of the CMT2Z patients detected throughout Spain is presented, accounting for one of the largest clinical series to date. This comprehensive phenotypic description allows the clinical and genetic spectrum of this disease to be delineated. The description of disease-causing *MORC2* variants is relatively recent and current reported patients are detailed in Table S1.

The most frequent underlying mutation is the p.R252W change, which was detected in one-third of the index cases in our series and 41% of those published, and affects the GHL-ATPase domain, where 9/18 of the causative *MORC2* mutations have been described. Three pathogenic novel mutations (p.R319C, p.A406V and p.D466G) and one VUS (p.A152P) were detected in our series; the latter also affects the ATPase domain. The p.R319C affects the coil–coil domain whilst the other two (p.A406V and p.D466G) are located in the transducer S5-like domain between the coil–coil and the zinc finger domain. This domain seems to be a hotspot for mutations as eight other changes in this location had already been reported to cause disease (Figure 1). In any case, there does not seem to be a clear correlation between the affected domain and the phenotypic spectrum, as changes in the same domain, or even in the same position as p.R132C and p.R132L, may cause quite different clinical presentations.

The phenotypic spectrum of these mutations includes both neuromuscular and central nervous system (CNS) impairment (Figure 1, Table S1). An attempt was made to delineate phenotypic categories according to the predominant feature (CNS neurodevelopmental vs. neuromuscular) and the muscle weakness distribution. The most distinctive clinical presentation was perhaps the scapuloperoneal phenotype which in our series corresponds to the patients with the p.R252W, p.A406V and p.D466G changes.

This group had a symptom onset in the first two decades with distal lower limb weakness and frequent cramps. Weakness spread early onto the distal upper limbs and subsequently to pelvic and shoulder girdle muscles, and neck extensors, whilst knee and elbow extensors were relatively preserved (Figure 2). Visible spontaneous muscular activity in proximal upper limb muscles was quite frequent (Videos), as were foot deformities (pes cavus and Achilles tendon shortening) and sensory impairment from an early age. CNS signs like hyperreflexia, learning difficulties or seizures which had previously been reported [2] were not detected.

There are other CMT subtypes with asymmetric muscle weakness, like the newly described repeat expansion in *VWA1*, but the combination of early proximal upper limb involvement and frequent spontaneous muscular activity with clear sensory impairment make this phenotypic subtype quite characteristic [24]. It is hypothesized that it may fit the description published by Davidenkow in 1927 and named scapuloperoneal amyotrophy [23]. He described sporadic and dominant families with 'a peculiar form of Charcot–Marie disease with typical distribution of atrophy in the lower limbs… on the other hand the atrophy of the upper extremities was localized proximally and involved the muscles of the shoulder girdle and partially those of the humerus, whilst hypesthesia showed a characteristic distal distribution'.

The muscle MRI in this clinical group revealed a recognizable pattern of fatty substitution and atrophy concordant with the clinical examination. There was preference of fatty infiltration in the calf muscles over the intrinsic foot muscles and asymmetry between muscle groups, being more prominent in the anterolateral and superficial posterior compartment in the calf, in certain muscles of the thigh (semimembranosus and semitendinosus) and shoulder girdle (deltoideus, trapezius and subscapularis), whilst mostly sparing the anterolateral compartment of the thigh and the adductor muscles. In any case these findings need to be replicated and extended to include patients who represent the whole phenotypic spectrum of *MORC2* mutations.

In the patients harbouring two other missense mutations (p.A152P and p.R319C) the predominant feature was also neuromuscular, but weakness appeared with a more typical length dependent distribution, more concordant with a classic CMT2 phenotype. Proximal weakness was symmetric and appeared only in the lower limbs and late in the course of the disease. Both had important sensory impairment, one of them with disabling walking instability and the other with upper limb tremor. The muscle MRI performed in one of these patients confirmed the length dependent distal predominance.

On the other hand, two patients developed a severe form of the disease with prominent neurodevelopmental and neuromuscular impairment. The p.S87L change has been described in four other patients who also presented with hypotonia and muscle weakness at birth, developing generalized weakness and sensory impairment [4,12]. Intellectual disability and facial dysmorphism were not detected in our patient but have been previously associated with this mutation [12]. The p.Y394C change is a clear example of the

14681331, 2021, 9, Downloaded from https://onlinelibrary.wiley.com/doi/10.1111/ene.15001 by Readcube (Labtiva Inc.), Wiley Online Library on [26/06/2023]. See the Terms and Conditions (https://onlinelibrary.wiley.com/terms-and-conditions) on Wiley Online Library for rules of use; OA articles are governed by the applicable Creative Commons License

phenotypic variability and overlap between the different phenotypic groups. Our patient presented with developmental motor delay and intellectual disability associated with prominent progressive weakness, being wheelchair bound since his 30s, but this same change has been previously described as a VUS in a sporadic Japanese patient with mild neuropathic features, and subsequently in two sporadic patients, one with prominent progressive, asymmetric limb weakness and elevated CK levels, and the other with a mild intellectual disability, hypoacusia and spasticity [10,12].

Nerve conduction studies confirmed an unequivocally axonal sensory and motor neuropathy irrespective of clinical categories or genotypes. Sensory lower limb nerves were severely affected even in patients with mild motor conduction abnormalities; in fact the lower limb SNAPs were not recordable or were severely reduced throughout the series. CMAP reduction was heterogeneous, being more pronounced in the peroneal nerve compared to the tibial nerve, which is concordant with the pattern of fatty infiltration detected in the calf muscle MRI of most scapuloperoneal patients. Needle electromyography revealed frequent spontaneous muscular activity predominantly in upper limb muscles, and this may be related to the frequently increased serum CK levels. Although the early proximal involvement and CK elevation may raise the issue of concomitant muscular damage, an in-depth review of the electrophysiological and pathological features of muscle and nerve biopsies in our patients and those reported so far reveal an unequivocal neuropathic injury [1,2,6,10].

MORC2 is a ubiquitous protein that has been shown to be highly expressed in both embryonic and adult human neural tissues, as well as in glia [15,16]. Loss of function murine models of Morc2 are lethal, with clear abnormalities in neural system development (https://dmdd.org.uk/mutants/Morc2a), and Morc2 expression has been seen to peak at early stages of development which is concordant with the neurodevelopmental features described in some patients [16]. Although there have been advances in understanding the way in which MORC2 dysfunction can alter neural development or produce neuron damage, the complete physiopathological mechanisms by which some *MORC2* changes alter the protein function in the early stages of neural development whilst others occur in a more mature nervous system are still to be clarified, and this may be one of the keys to better understand the phenotypic spectrum in this disease.

ACKNOWLEDGEMENTS

The commitment of the families studied is deeply appreciated.

DISCLOSURES

None.

AUTHOR CONTRIBUTIONS

Rafael Sivera: Conceptualization (equal); data curation (lead); formal analysis (equal); funding acquisition (supporting); investigation (equal); methodology (equal); validation (equal); visualization (equal); writing—original draft (lead); writing—review and editing (equal). Vincenzo Lupo: Data curation (equal); investigation (equal); methodology (lead); software (equal); writing—review and editing (equal). Marina Frasquet: Data curation (equal); formal analysis (equal); writing—review and editing (equal). Herminia Argente-Escrig: Data curation (equal); formal analysis (equal); writing—review and editing (equal). Jorge Alonso-Pérez: Data curation (equal); formal analysis (equal); writing—review and editing (equal). Jordi Diaz-Manera: Data curation (equal); formal analysis (equal); writing—review and editing (equal). Luis Querol: Data curation (equal); formal analysis (equal); writing—review and editing (equal). Maria del Mar García-Romero: Data curation (equal); formal analysis (equal); writing—review and editing (equal). Samuel Ignacio Pascual-Pascual: Data curation (equal); formal analysis (equal); writing—review and editing (equal). Tania García-Sobrino: Data curation (equal); formal analysis (equal); writing—review and editing (equal). Carmen Paradas: Data curation (equal); formal analysis (equal); writing—review and editing (equal). Juan Francisco Vázquez Costa: Data curation (equal); formal analysis (equal); writing—review and editing (equal). Nuria Muelas Gómez: Data curation (equal); formal analysis (equal); writing—review and editing (equal). Elvira Millet: Data curation (equal); formal analysis (equal); writing—review and editing (equal). Juan J Vílchez: Data curation (equal); formal analysis (equal); writing—review and editing (equal). Carmen Espinós: Data curation (equal); formal analysis (equal); writing—review and editing (equal). Teresa Sevilla: Conceptualization (lead); funding acquisition (equal); project administration (equal); supervision (lead); validation (equal); writing—original draft (equal); writing—review and editing (lead).

DATA AVAILABILITY STATEMENT

The data that support the findings of this study are available from the corresponding author upon reasonable request.

ORCID

Rafael Sivera https://orcid.org/0000-0003-2810-1180
Vincenzo Lupo https://orcid.org/0000-0002-3774-9854
Marina Frasquet https://orcid.org/0000-0001-7206-5362
Herminia Argente-Escrig https://orcid.org/0000-0001-8537-1318
Jorge Alonso-Pérez https://orcid.org/0000-0001-8866-5186
Tania García-Sobrino https://orcid.org/0000-0001-8067-431X
Juan Francisco Vázquez-Costa https://orcid.org/0000-0002-3043-7938
Nuria Muelas https://orcid.org/0000-0002-2349-7481
Carmen Espinós https://orcid.org/0000-0003-4435-1809
Teresa Sevilla https://orcid.org/0000-0003-4716-2667

REFERENCES

1. Sevilla T, Lupo V, Martinez-Rubio D, et al. Mutations in the *MORC2* gene cause axonal Charcot–Marie–Tooth disease. *Brain*. 2016;139:62-72.
2. Albulym OM, Kennerson ML, Harms MB, et al. *MORC2* mutations cause axonal Charcot–Marie–Tooth disease with pyramidal signs. *Ann Neurol*. 2016;79:419-427.
3. Lassuthova P, Safka-Brozkova D, Krutova M, et al. Severe axonal Charcot–Marie–Tooth disease with proximal weakness caused by de novo mutation in the *MORC2* gene. *Brain*. 2016;139:e26.

14681331, 2021, 9, Downloaded from https://onlinelibrary.wiley.com/doi/10.1111/ene.15001 by Readcube (Labtiva Inc.), Wiley Online Library on [26/06/2023]. See the Terms and Conditions (https://onlinelibrary.wiley.com/terms-and-conditions) on Wiley Online Library for rules of use; OA articles are governed by the applicable Creative Commons License

4. Hyun YS, Hong YB, Choi BO, Chung KW. Clinico-genetics in Korean Charcot–Marie–Tooth disease type 2Z with *MORC2* mutations. *Brain*. 2016;139:e40.
5. Zhao X, Li X, Hu Z, et al. *MORC2* mutations in a cohort of Chinese patients with Charcot–Marie–Tooth disease type 2. *Brain*. 2016;139:e56.
6. Schottmann G, Wagner C, Seifert F, Stenzel W, Schuelke M. *MORC2* mutation causes severe spinal muscular atrophy-phenotype, cerebellar atrophy, and diaphragmatic paralysis. *Brain*. 2016;139:e70.
7. Semplicini C, Ollagnon-Roman E, Leonard-Louis S, et al. High intrafamiliar clinical variability in *MORC2* mutated CMT2 patients. *Brain*. 2017;140:e21.
8. Zanni G, Nardella M, Barresi S, et al. De novo p.T362R mutation in *MORC2* causes early onset cerebellar ataxia, axonal polyneuropathy, and nocturnal hypoventilation. *Brain*. 2017;140(6):e34. https://doi.org/10.1093/brain/awx083
9. Bansagi B, Griffin H, Whittaker RG, et al. Genetic heterogeneity of motor neuropathies. *Neurology*. 2017;88:1226-1234.
10. Ando M, Okamoto Y, Yoshimura A, et al. Clinical and mutational spectrum of Charcot–Marie–Tooth disease type 2Z caused by MORC2 variants in Japan. *Eur J Neurol*. 2017;24:1274-1282.
11. Karakaya M, Storbeck M, Strathmann EA, et al. Targeted sequencing with expanded gene profile enables high diagnostic yield in non-5q-spinal muscular atrophies. *Hum Mutat*. 2018;39:1284-1298.
12. Guillen Sacoto MJ, Tchasovnikarova IA, Torti E, et al. De novo variants in the ATPase module of MORC2 cause a neurodevelopmental disorder with growth retardation and variable craniofacial dysmorphism. *Am J Hum Genet*. 2020;107:352-363.
13. Inoue N, Hess KD, Moreadith RW, et al. New gene family defined by MORC, a nuclear protein required for mouse spermatogenesis. *Hum Mol Genet*. 1999;8:1201-1207.
14. Iyer LM, Abhiman S, Aravind L. MutL homologs in restriction-modification systems and the origin of eukaryotic MORC ATPases. *Biol Direct*. 2008;3:8.
15. Douse CH, Bloor S, Liu Y, et al. Neuropathic *MORC2* mutations perturb GHKL ATPase dimerization dynamics and epigenetic silencing by multiple structural mechanisms. *Nat Commun*. 2018;9:651.
16. Sancho P, Bartesaghi L, Miossec O, et al. Characterization of molecular mechanisms underlying the axonal Charcot–Marie–Tooth neuropathy caused by *MORC2* mutations. *Hum Mol Genet*. 2019;28:1629-1644.
17. Richards S, Aziz N, Bale S, et al. Standards and guidelines for the interpretation of sequence variants: a joint consensus recommendation of the American College of Medical Genetics and Genomics and the Association for Molecular Pathology. *Genet Med*. 2015;17:405-424.
18. Shy ME, Blake J, Krajewski K, et al. Reliability and validity of the CMT neuropathy score as a measure of disability. *Neurology*. 2005;64:1209-1214.
19. Murphy SM, Herrmann DN, McDermott MP, et al. Reliability of the CMT neuropathy score (second version) in Charcot–Marie–Tooth disease. *J Peripher Nerv Syst*. 2011;16:191-198.
20. Muelas N, Frasquet M, Más-Estelles F, et al. A study of the phenotypic variability and disease progression in Laing myopathy through the evaluation of muscle imaging. *Eur J Neurol*. 2020. https://doi.org/10.1111/ene.14630
21. Fischer D, Kley RA, Strach K, et al. Distinct muscle imaging patterns in myofibrillar myopathies. *Neurology*. 2008;71:758-765.
22. Kyriakides T, Angelini C, Schaefer J, et al. EFNS guidelines on the diagnostic approach to pauci- or asymptomatic hyperCKemia. *Eur J Neurol*. 2010;17:767-773.
23. Davidenkow S. IJber die neurotische Muskelatrophie Charcot–Marie. *Klinisch-genetische Studien. Neur U Psych*. 1927;107:259-320.
24. Pagnamenta AT, Kaiyrzhanov R, Zou Y, et al. An ancestral 10-bp repeat expansion in *VWA1* causes recessive hereditary motor neuropathy. *Brain*. 2021;144:584-600.

SUPPORTING INFORMATION

Additional supporting information may be found online in the Supporting Information section.

How to cite this article: Sivera R, Lupo V, Frasquet M, et al. Charcot–Marie–Tooth disease due to *MORC2* mutations in Spain. *Eur J Neurol*. 2021;28:3001–3011. https://doi.org/10.1111/ene.15001

14681331, 2021, 9, Downloaded from https://onlinelibrary.wiley.com/doi/10.1111/ene.15001 by Readcube (Labtiva Inc.), Wiley Online Library on [26/06/2023]. See the Terms and Conditions (https://onlinelibrary.wiley.com/terms-and-conditions) on Wiley Online Library for rules of use; OA articles are governed by the applicable Creative Commons License